JOURNAL OF MATERIALS SCIENCE 32 (1997) 4507–4512

Nanostructured and near defect-free ceramics by low-temperature pressureless sintering of nanosized Y-TZP powders

P. DURÁN, M. VILLEGAS, F. CAPEL, J. F. FERNÁNDEZ, C. MOURE
Instituto de Cerámica y Vidrio (CSIC), Electroceramics Department, 28500 Arganda del Rey, Madrid, Spain

Nanosized (~6 nm) Y-TZP (3 mol % Y_2O_3) powders have been produced by chemical co-precipitation (Y-inorganic + Zr-organic precursors) and thorough isopropanol-washing step, after calcining in air at 450 °C. The nanocrystalline Y-TZP powders consisted of spherical soft agglomerates (~100 nm in size) which were easily broken down during compaction resulting in a very uniform green microstructure with a narrow pore size distribution (average pore size less than 6.5 nm) and no detectable compacting defects. In spite of the relatively low green density (43% theoretical), Y-TZP powder compacts sintered to near theoretical density in the very low-temperature range of 1000 °C for 80–100 h to 1070 °C for 2 h, maintaining a grain size in the nanoscale (<100 nm) and the sintered bodies were nearly defect-free. Hardly any grain growth took place up to 1000 °C; it was very rapid above this temperature.

1. Introduction

The retention of fine-scale microstructures in sintered bodies is very useful for certain material properties such as strength, fracture toughness, and ionic conductivity [1–3]. Decreasing grain size improves both bending strength and fracture toughness, and if the grain size is reduced to the nanocrystalline range then superplastic forming is feasible which is, in some cases, preferable to pressureless sintering because it gives better microstructural control [4–6]. However, nanometre-sized particles are rich in internal defects that, on compacting, will be present in the green microstructure. During sintering they will grow and their effect on properties will become more evident.

Since the strength of ceramic materials is sensitive to the presence of defects, and these are induced by green microstructure inhomogeneities, the prevention of any gradient in green density, homogeneity, agglomeration and particle size will lead to a high density, fine microstructure, and defect-poor or defect-free sintered products [7–9]. Therefore a deep knowledge of the pore size distribution, chemical homogeneity, and density gradients in green compacts is necessary to ensure uniform sintering.

In the specific case of zirconia ceramics, special requirements have to be satisfied by the powders used in obtaining nanostructured and defect-free sintered bodies. For example, the powders must have a well controlled size, size distribution, shape, and agglomeration state. When these powder requirements are achieved then compacts having uniform green microstructure, especially with a narrow pore size distribution, and defect-free sintered bodies could be attained [10]. Although there are some problems with small particles related to their agglomeration tendency, this difficulty could be overcome with reversible agglomeration and deagglomeration characteristics of the powder. If this is so, then the powder will have a small size which is defect-free in the deagglomerated state and will exhibit homogeneous packing and an improved sintering response.

Although many techniques, such as hydrolysis of metal alkoxides [11, 12], co-precipitation from aqueous solution [13, 14], hydrothermal reaction [15], and more recently the inert gas condensation method [8], have been developed to prepare yttria-doped tetragonal zirconia (Y-TZP) ultrafine (nanocrystalline) powders, difficulties with most of them, mainly in cost and control of the composition, preclude their utilization. Gel-precipitation from aqueous and/or alcoholic solutions seems to be a more promising route for making nanocrystalline Y-TZP powders [14–16]. On this basis, the present work was carried out to study the influence of the synthesis method and the powder processing on the powder characteristics, microstructure of the green compacts and the sintering behaviour of the nanocrystalline powders obtained.

2. Experimental procedure

A 3 mol % Y_2O_3–ZrO_2 produced by a co-precipitation method was used in this study. An isopropanol solution containing yttrium and zirconium cations was added to an isopropanol–water ammonium hydroxide solution by stirring. At the end of the co-precipitation process a white co-precipitate of

0022–2461

zirconium and yttrium hydroxides was obtained. The co-precipitate was filtered and thoroughly washed with isopropanol and then air calcined at 450 °C for 5 h to produce the yttria-doped zirconia oxide. The details of the powder preparation are reported elsewhere [17]. The only differences were a thorough isopropanol-washing step and a lower calcining temperature.

Co-precipitated isopropanol washed (IW) and calcined powders were characterized by differential thermal analysis/thermogravimetric analysis (DTA/TG), and by Fourier transform infrared (FTIR) spectrometry. Specific surface areas were calculated by the Brunauer–Emmett–Teller (BET) method. Crystallite sizes of calcined powders were determined by the X-ray line broadening (Scherrer) method. Particle size and shape were also examined by both transmission (TEM) and scanning (SEM) electron microscopy. Green compacts of the IW-calcined powder were produced at different compaction pressures up to 350 MPa and their compaction behaviour was studied by measuring the changes in density. The pore size distributions in green compacts (200 MPa) were studied by mercury porosimetry. Non-isothermal sintering (CHR) behaviour was studied using a heating rate of 120 °C h^{-1} to 1400 °C. Isothermal sintering was carried out at 1000 to 1150 °C several times. The densities of the sintered samples were determined by the Archimedes method. Virgin surfaces of the sintered samples as well as polished and fractured surfaces were examined by SEM, and the grain sizes of the sintered samples were measured by X-ray line broadening or by the interception method [18].

3. Results and discussion

The co-precipitated IW powder consisted of almost spherical agglomerates and a specific surface area as high as 290 $m^2 g^{-1}$ was measured. After calcining, as shown in Fig. 1, a loose agglomerated powder was obtained. It seems that during the isopropanol-washing step the adsorption of isopropanol on the hydroxyl group surfaces of the hydrous zirconia inhibits the formation of bridging between neighbouring precipitate particles, thus impeding the formation of hard agglomerates during the drying process and, therefore, improving the sinterability of the Y-TZP powders [19, 20]. The morphology of these agglomerates, about 100 nm in size, was quite similar to the co-precipitated one but the surface area, as measured with BET, decreased to 140 $m^2 g^{-1}$. Nitrogen adsorption isotherms obtained from the loose powder revealed that the pore size was in the range of $\sim$20 nm. The primary crystalline size, as determined by X-ray line broadening, was about 6 nm. Consistent results, about 8 nm, also were obtained by TEM, see Fig. 2. The calculated specific surface of the isolated Y-TZP particles is $\sim$165 $m^2 g^{-1}$. These results indicate that the agglomerates have both a high internal porosity and a substructure consisting of many smaller particles.

It is visualized, from Fig. 2, that the loose nanosized Y-TZP powder is formed by three kinds of micro-

Figure 1 SEM photograph of IW-air calcined Y-TZP nanosized powders showing almost spherical agglomerates.

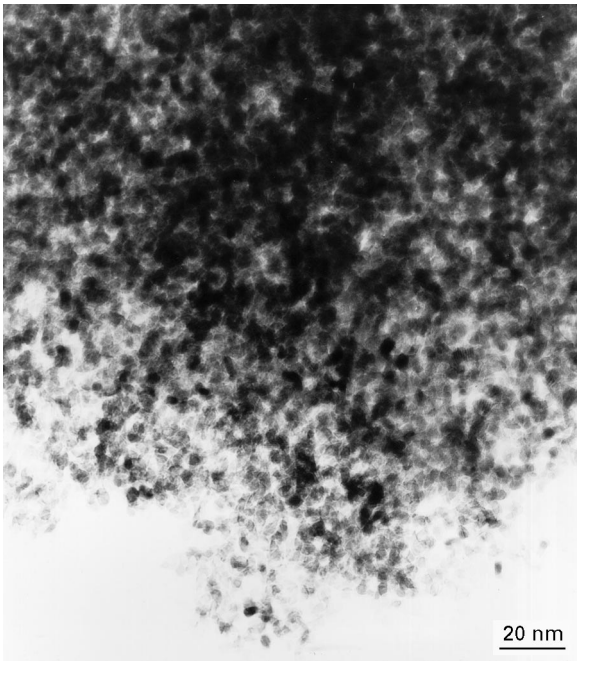

Figure 2 TEM photograph of loose nanosized Y-TZP powder.

structural subunits with different sizes: (a) the first are the primary crystallites ($\leqslant$6 nm); (b) the second are formed by aggregates or domains with a very uniform distribution size (15–20 nm in diameter) constituted by several primary crystallites linked by necks; and (c) the third kind are agglomerates with irregular shape (less than 100 nm in size), formed by the union of some domains (3 to 6) held together like chains by weak attractive forces. The phase analysis by X-ray diffraction revealed that the IW co-precipitate was amorphous and a relatively well crystallized tetragonal zirconia without traces of other phases was formed after calcining.

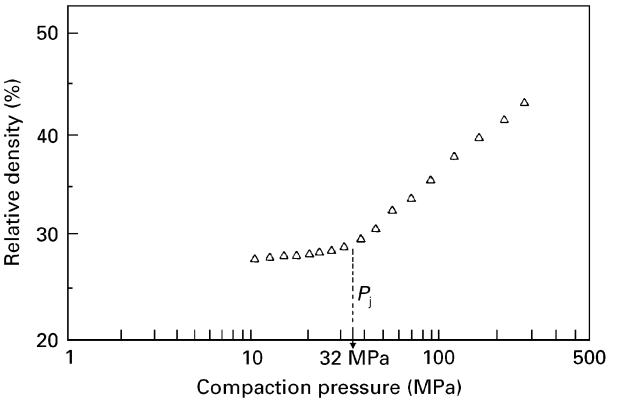

Figure 3 Compaction behaviour of nanosized Y-TZP powders.

Fig. 3 shows the compaction behaviour of the nanosized Y-TZP powders. The relative densities of the green compacts were plotted as a function of the logarithm of the applied isopressure. A curve with two well defined linear parts intersected at a pressure P_j was obtained. The lower P_j is, the lower is the strength of the agglomerates. A value of P_j as low as 32 MPa was found which is much lower than those reported for Y-TZP powders obtained by different methods [16]. If the porosity of the agglomerates also gives an indication of the agglomerates' strength [21], then it should be assumed that, as mentioned above, the internal porosity of the agglomerates in the IW-calcined powders was quite high. These spherical and porous agglomerates showed a good packing capability and can be easily broken during compaction giving rise to a homogeneous distribution of both the stresses and the density in the green compacts.

The above statement is corroborated by the absence of any sharp edges of density inhomogeneities in the green bodies as shown in Fig. 4. If any defects had been introduced during the compacting process they were not detected in the green state even at higher electron micrograph magnifications. Thus it can be concluded that, as a consequence of the isopropanol-washing step, the quasi-spherical and small agglomerates in the nanosized-Y-TZP powders were porous and mechanically soft. Hence, the friction between agglomerates was very low, thus leading to a homogeneous green microstructure after compaction.

Taking into account the different microstructural subunits present in the loose nanosized Y-TZP powder, and its compaction behaviour depicted in Fig. 4, we could also hypothesize the existence of several types of pores contributing to the total porosity in the nanosized Y-TZP powder compacts, as follows: (i) pores between the particles within a domain/aggregate or intra-domain porosity, and it would be constituted by the pores having the lowest coordination; (ii) those pores located between domains/aggregates or inter-domain (also named intra-agglomerate) porosity; and finally (iii) the pores between the agglomerates or inter-agglomerate porosity. The pore coordination in the inter-agglomerate porosity would be, of course, higher than that of the pores in the inter-domain or intra-agglomerate porosity [22].

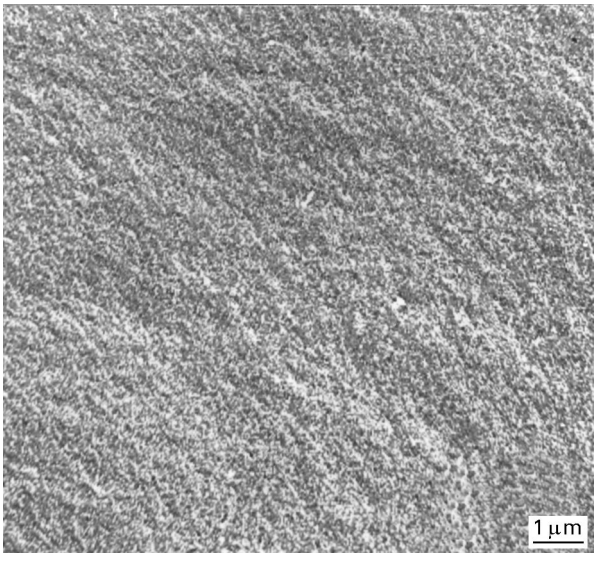

Figure 4 Green microstructure of nanosized Y-TZP powder compacts.

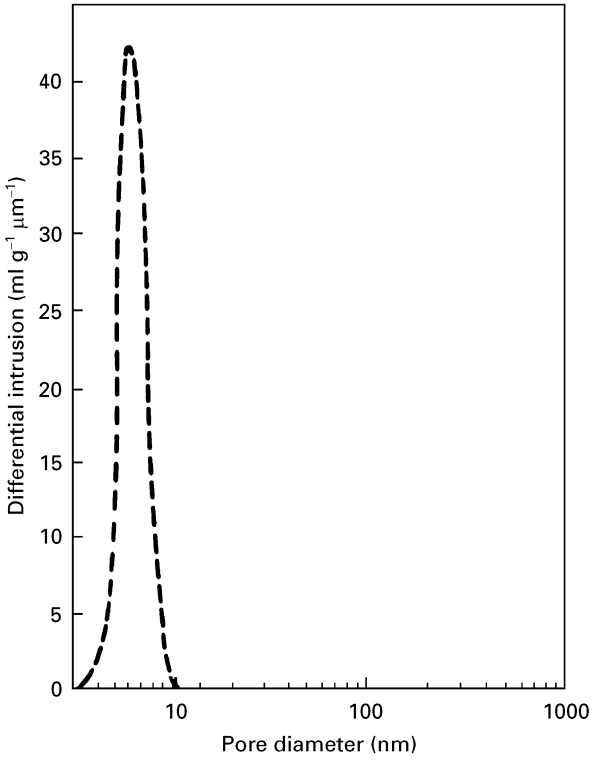

Figure 5 Pore size distribution of nanosized Y-TZP green compacts.

The pore size distribution in compacts after isopressing at 200 MPa is given in Fig. 5. The nanosized-Y-TZP powder compacts have a narrow pore size distribution with a single peak located at a pore diameter of 6.5 nm. The asymmetrical pore size distribution curve could be indicating the presence of a certain amount of smaller pores (diameter less than 3 nm) in the nanosized-Y-TZP green compacts. No large pores (>10 nm) were found in the green microstructure. This fact indicates that during the compaction the average interparticle distance is decreased and, thus, the pore size distribution is displaced towards smaller pore diameters leading to green compacts with

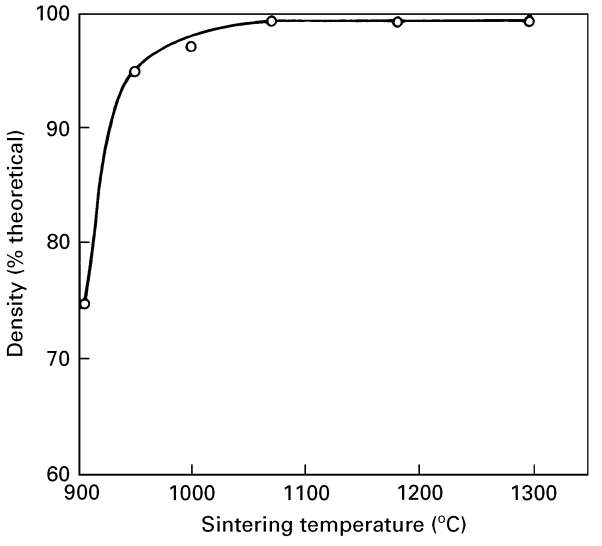

Figure 6 Density of nanosized Y-TZP samples as a function of sintering temperature. Soaking time was 5 h.

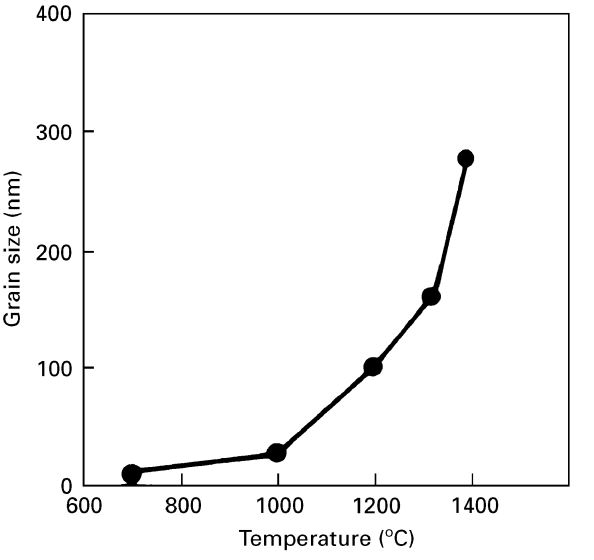

Figure 7 Grain size of nanosized Y-TZP samples as a function of sintering temperature (hold time, 2 h).

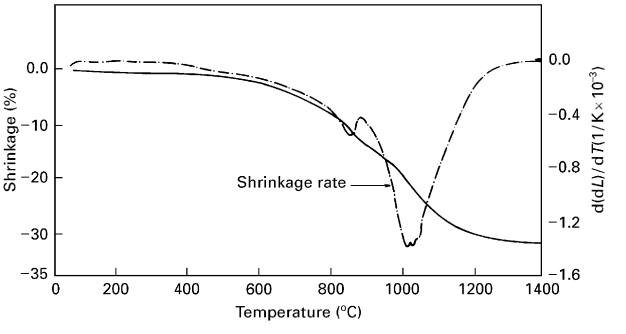

Figure 8 Non-isothermal sintering behaviour of nanosized Y-TZP green compacts.

intra- and interagglomerate pores of almost the same dimensions. Accordingly it should be also assumed that there is both an increase in the particle coordination number and a decrease in the pore coordination number. If this is so, then the densification rate should be enhanced [22].

Fig. 6 shows the sintering temperature dependence of density for nanosized-Y-TZP sintered samples. Although the green density was as low as 43% of the theoretical density, very far from that considered as near-ideal close packing ($\sim$78% theoretical), the samples exhibited a 95% density at temperatures as low as 950 °C, and were theoretically dense at 1070 °C. These high densities could be a consequence of several combined factors: (i) the large surface area to volume ratio of the nanosized-Y-TZP powders; (ii) the increase of both the surface forces and the sintering pressure acting to enhance densification [23]; and finally, (iii) the very homogeneous green structure which, in spite of the low green density, lead to high densification [13].

Although some grain growth during the densification process is inevitable, in the sintered samples of the Fig. 6, the grains have grown to about 38 nm at 1000 °C which is 6 times the initial particle size, and only up to 86 nm at 1070 °C for the theoretically dense samples. At 1400 °C (with no soaking sintering time) the grain size was still 215 nm. Fig. 7 shows the grain size variation with temperature for a hold time of 2 h. As can be observed, the grain size slowly increases up to $\sim$1000 °C and above this temperature grain growth rapidly increases.

Fig. 8 shows the non-isothermal sintering curves of nanosized Y-TZP compacts. Shrinkage begins at temperatures as low as 500 °C, and above this temperature shrinkage was linear and continuous up to the hold temperature. The final density is achieved at a temperature somewhat higher than 1200 °C. The same figure shows the shrinkage rate as a function of densification temperature. Two maxima were found, one of them at about 800 °C and a higher peak in the shrinkage rate follows at approximately 1000 °C. Each of them seems to correspond to a type of pore in the pore-size distribution curve. The smaller pores ($<$3 nm), probably intra-agglomerates, are eliminated at the lower temperatures and the larger, interagglomerates, need higher temperatures to be eliminated [24, 25]. Both the speed and low temperature (much lower than $0.5T_m$) of pore elimination confirm the homogeneous porosity distribution in the nanosized-Y-TZP green compacts, as shown in Fig. 5.

Although the small particle size, but not monosized, could not be the only condition to achieve high densification, the fact that near theoretically dense bodies were obtained at temperatures as low as 1000–1070 °C, see Fig. 6, indicates that a high particle coordination number and uniform packing exist in the nanosized-Y-TZP green compacts in spite of the relatively low green density [23]. On the other hand, the fast elimination of the pores allows us to state that the pore coordination number in the nanosized-Y-TZP green compacts was below the critical value (R_c), for pores to disappear by volume/grain boundary diffusion [26, 27]. Furthermore, since the particle size of the Y-TZP powder is very small (nanometric characteristics) then a large generated sintering pressure and an assumed small variation in the particle coordination number, lead to both an enhanced shrinkage rate

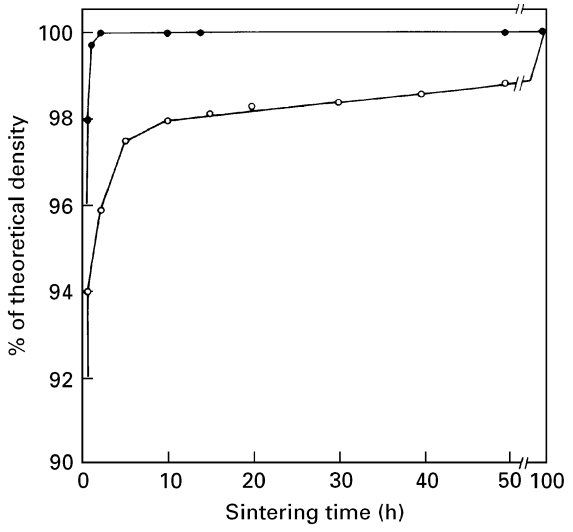

Figure 9 Isothermal sintering behaviour of nanosized Y-TZP green compacts: ● 1070 °C and ○ 1000 °C.

and a complete densification at low temperature [1, 28, 29]. Although such a sintering pressure could finally result in the formation of flaws in the sintered bodies, the absence of both hard agglomerates or large pores in the nanosized-Y-TZP green compacts, see Fig. 4, leads to fully densified almost defect-free bodies maintaining a grain size less that 100 nm (nanostructured) being achieved by pressureless sintering at very low temperatures. It means that Y-TZP nanostructured ceramics could be achieved below 1000 °C with adequate powder processing. Thus a Y-TZP unagglomerated powder with higher surface energy (higher surface/volume ratio) could potentially lead to fully dense bodies by reducing the solid surface curvature and delivering more free energy from the system.

Given that the major densification took place at 1000 to 1100 °C, dense bodies with small grain sizes could be obtained in that temperature range, thus temperatures of 1000 and 1070 °C were chosen for the isothermal sintering studies. Fig. 9 shows the isothermal sintering curves of the samples sintered at 1000 and 1070 °C. Starting with 43% green density, the samples can sinter to full density ($\geqslant$99.9% theoretical) with a grain size of only 72 nm after 2 h holding time at 1070 °C. When the sintering peak of 1000 °C is used then the samples take 80–100 h to reach full density but the grain size is still less than 100 nm. The little grain growth observed at this point indicates that the mobility of the pores was much higher than that of the grain boundaries and, hence, they would have a pinning effect on the grain growth process. Fig. 10 shows the polished and thermally etched surface of a 99.9% dense sample. Uniformity in density is achieved and the fine particulate nanostructure, is maintained. This microstructure of grains with well-developed grain boundaries and no detectable residual porosity is typical of a ceramic body in the final sintering stage. In contrast, SEM observations on the polished cross-section and non-etched surface sample showed some residual porosity that was not eliminated, although no structural defects (crack-like voids) were detected. Therefore, it has been demonstrated

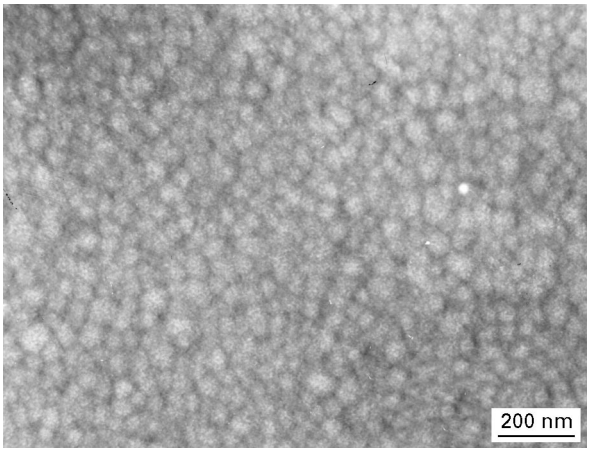

Figure 10 SEM of nanosized Y-TZP 99.9% dense samples.

with these isothermal experiments that after 2 h sintering at a temperature as low as 1070 °C, Y-TZP dense bodies with a grain size in the nanoscale range and, apparently, defect-free can be achieved. Similar results were obtained in the case of a nanocrystalline TiO_2 prepared by an inert gas condensation technique [7], but nanostructured Y-TZP could not be prepared [30].

4. Conclusions

The above described experimental results allow us to draw the following conclusions.

1. Nanoparticles of Y-TZP with an average grain size of 6 nm can be produced by calcining at 450 °C, a thoroughly isopropanol-washed co-precipitated amorphous Y-TZP powder.

2. The obtained nanosized Y-TZP powder contained soft agglomerates, $\sim$100 nm in diameter, which were easily fragmented during compaction leading to green compacts with a very uniform microstructure, a narrow pore size distribution (only maximum at a pore size smaller than 8 nm), and with very few defects or defect-free.

3. The unique characteristics of such nanosized powder compacts allowed fully dense bodies of Y-TZP with a grain size in the nanoscale ($<$100 nm) and near defect-free by pressureless sintering at a temperature as low as 1000 °C for 80–100 h or 1070 °C for 2 h, to be achieved.

Acknowledgement

This work was supported by CICYT-MAT-94-871.

References

1. R. J. BROOK, *Proc. Br. Ceram. Soc.* **32** (1982) 7.
2. G. S. A. M. THEUNISSEN, J. S. BOUMA, A. J. A. WINNUNST and A. J. BURGGRAAF, *J. Mater. Sci.* **27** (1992) 4429.
3. G. S. A. M. THEUNISSEN, PhD thesis, University of Twente, Enschede, The Netherlands (1991).
4. F. WAKAI, S. SAKAGUCHI and Y. MATSUNO, *Adv. Ceram. Mater.* **1** (1986) 259.
5. H. HAHN and R. S. AVERBACK, *J. Amer. Ceram. Soc.* **74** (1991) 2918.

6. M. M. R. BOUTZ, A. J. A. WINNUBST, A. J. BURGGRAAF, M. NAUER and C. CARRY, *ibid.* **78** (1995) 121.
7. H. HAHN, J. LOGAS and R. S. AVERBACK, *J. Mater. Res.* **5** (1990) 609.
8. R. W. SIEGEL, S. RAMASAMY, H. HAHN, Z. LI and R. GRONSKY, *ibid.* **3** (1988) 1367.
9. C. D. SAGEL-RANSIJN, A. J. A. WINNUBST, B. KERRWIJK, A. J. BURGGRAAF and H. VERWEIJ, *J. Europ. Ceram. Soc.* (1996) in press.
10. P. C. PANDA, J. WANG and R. RAJ, *J. Amer. Ceram. Soc.* **71** (1988) C-507.
11. K. S. MAZDIYASNI, C. T. LYNCH and J. S. SMITH, *ibid.* **48** (1965) 372.
12. *Idem*, *ibid.* **49** (1966) 286.
13. K. HABERKO, *Ceram. Int.* **5** (1979) 148.
14. W. F. M. GROOT ZEVERT, A. J. A. WINNUBST, G. S. A. THEUNNISSEN and A. J. BURGGRAAF, *J. Mater. Sci.* **25** (1990) 3449.
15. E. TANI, M. YOSHIMURA and S. SOMIYA, *J. Amer. Ceram. Soc.* **64** (1981) C-8.
16. M. A. C. G. VAN DER GRAAF and A. J. BURGGRAAF, in "Advances in Ceramics", Vol. 12, Science and Technology of Zirconia II, edited by N. Claussen, M. Ruhle and H. Heuer (American Ceramic Society, Columbus, OH, 1984) pp. 744–65.
17. P. DURAN, M. VILLEGAS, F. CAPEL, P. RECIO and C. MOURE, *J. Europ. Ceram. Soc.* **16** (1996) 945.
18. R. L. FULLMAN, *J. Metals. Trans. AIME* **197** (1953) 447.
19. P. RECIO, C. PASCUAL, C. MOURE, J. R. JURADO and P. DURAN, *Brit. Ceram. Proc.* **38** (1987) 127.
20. M. S. KALISZEWSKI and A. H. HEUER, *J. Amer. Ceram. Soc.* **73** (1990) 1504.
21. M. A. C. G. VAN DER GRAAF, J. H. H. TER MAAT and A. J. BURGGRAAF, *J. Mater. Sci.* **20** (1985) 1407.
22. F. F. LANGE, *J. Amer. Ceram. Soc.* **67** (1984) 83.
23. E. G. LINIGER and R. RAJ, *ibid.* **71** (1988) C-408.
24. R. PAMPUCH and K. HABERKO, in "Ceramic Powders", edited by P. Vincenzini (Elsevier Science Publishers, Amsterdam, 1983).
25. A. ROOSEN and H. HAUSNER, in "Advances in Ceramics", Vol. 12, Science and Technology of Zirconia II, edited by N. Claussen, M. Ruhle and H. Heuer, (American Ceramic Society, Columbus, OH, 1984) pp. 714–26.
26. W. D. KINGERY and B. FRANCOIS, in "Sintering and Related Phenomena", edited by G. C. Kuczynski, N. A. Hooton and G. F. Gibbon, (Gordon and Breach, New York, 1967) pp. 471–98.
27. F. F. LANGE and B. I. DAVIS, in "Advances in Ceramics", Vol. 12, Science and Technology of Zirconia II, edited by N. Claussen, M. Ruhle and H. Heuer, (American Ceramic Society, Columbus, OH, 1984) pp. 699–713.
28. R. RAJ, *J. Amer. Ceram. Soc.* **70** (1987) C-210.
29. E. LINIGER and R. RAJ, *ibid.* **70** (1987) 843.
30. G. SKANDAN, H. HAHN, M. RODDY and W. R. CANNON, *ibid.* **77** (1994) 1706.

Received 22 November 1996
and accepted 10 February 1997